Carbonate content and stable isotopic composition of atmospheric aerosol carbon in the Canadian High Arctic

Petr Vodička[1,2], Kimitaka Kawamura[2], Bhagawati Kunwar[2,3], Lin Huang[4] , Dhananjay Kumar[2,a],

Md. Mozammel Haque[2,5], Ambarish Pokhrel[2], Sangeeta Sharma[4], Leonard Barrie[6]

[1] Institute of Chemical Process Fundamentals, Czech Academy of Sciences, 165 00 Prague 6, Czech Republic

[2] Chubu Institute for Advanced Studies, Chubu University, 1200 Matsumoto-cho, Kasugai 487–8501, Japan

[3] Institute for Space-Earth Environmental Research, Nagoya University, Nagoya 464-8601, Japan

[4] Environment and Climate Change Canada, Science and Technology Branch, 4905 Dufferin St., Toronto, Canada

[5] School of Ecology and Applied Meteorology, NUIST, Nanjing, 210044, China

[6] Atmospheric and Oceanic Sciences Department, McGill University, Montreal, Canada

[a] Now at: Commission for Air Quality Management in National Capital Region and Adjoining Areas, New Delhi 110001, India

Correspondence to: Petr Vodička (vodicka@icpf.cas.cz) and Kimitaka Kawamura (kkawamura@isc.chubu.ac.jp)

Abstract. The carbon cycle in the Arctic atmosphere is important in understanding abrupt climate changes occurring in this region. Two-years of measurements (summer 2016 - spring 2018) of carbonaceous aerosols at the High Arctic station Alert, Canada, showed that in addition to organic carbon (OC) and elemental carbon (EC), carbonate carbon (CC) was episodically but not negligibly present. The relative abundances of CC in total carbon (TC) ranged from 0-65 % with an average of approximately 11 % over the entire period. Also there was a strong correlation of CC with aerosol Ca^{2+} which is associated mostly with soil dust and to a lesser extent sea salt aerosol. Based on this and the analysis of air mass back trajectories (AMBT), we infer two possible sources of CC in the Arctic total suspended particles (TSP). The major one is the erosion and resuspension of limestone sediments, particularly in the semi-desert areas of the northern Canadian Arctic. Another potential minor source of CC is marine aerosol, including calcified marine phytoplankton shells (coccoliths) introduced into the atmosphere via sea-to-air emission.

The CC content significantly influenced the stable carbon isotopic composition ($\delta^{13}C$) of TC. The higher the CC content, the higher the $\delta^{13}C$ values, which is consistent with the strong ^{13}C enrichment in carbonates. Therefore, carbonates in Arctic TSP must be taken into account not only in isotopic studies using $\delta^{13}C$ analyses but also when assessing the impact of carbonaceous aerosols on the Arctic climate.

1 Introduction

The Arctic is a dynamically changing region that is significantly affected by climate change (England et al., 2021). Aerosols are one of the factors influencing the climate, but their effects are subject to significant uncertainties (Carslaw et al., 2013). The uncertainties in radiative forcing is primarily associated with carbonaceous aerosols, most of which is composed of organic carbon (OC). In contrast, a smaller fraction consists of elemental carbon (EC), which is equivalent to optically determined black carbon (BC) (Petzold et al., 2013).

Organic aerosols, i.e., OC in the atmosphere, generally have a cooling effect on the climate (Stjern et al., 2016) except for the part called brown carbon (Laskin et al., 2015). On the other hand, EC or BC has the warming effect, both in the atmosphere (Liu et al., 2020) and on snow surface (Flanner et al., 2007) especially important in the Arctic. In addition, EC and BC measurements are also used to determine the mass absorption cross section (MAC), a fundamental input to radiative transfer models (Mbengue et al., 2021). The MAC is season- and station- specific (Savadkoohi et al., 2024), making it one of the parameters in affecting the influence of aerosols on climate. If either EC or BC is determined inaccurately, the MAC factor will be subsequently biased as well (Chen et al., 2021). Therefore, detailed knowledge of the composition of carbonaceous aerosol in the Arctic is crucial for improving our understanding of their impacts on the climate changes in this region.

Recent atmospheric studies from Tajikistan (Chen et al., 2021) and Tibet (Hu et al., 2023) indicate a significant contribution of carbonates in total suspended particles (TSP), which may have a significant effect on the determination of OC and EC (or BC). Those areas are characterized as arid desert regions with sparse vegetation, large amounts of unconsolidated sediments, and lack of soil moisture, where the wind erosion plays an important role in the aeolian processes such as atmospheric transports and dust deposits. Arctic regions are affected by long range transport of dust and also contributed by dust locally (Groot Zwaaftink et al., 2016; Sharma et al., 2019; Sirois and Barrie, 1999). They have a desert, semi-desert or arid character in some cases (Pushkareva et al., 2016). Recently high-latitude dust sources have been described as a significant climate and environmental factor (Kawai et al., 2023; Kawamura et al., 1996; Meinander et al., 2022). It is reported that carbonate rich dust also has a slightly positive effect on radiative forcing, although lower than BC (Chen et al., 2021; Raman et al., 2011). High Arctic semi-desert aerosols have been described as potentially important reservoirs of soil organic matter (Muller et al., 2022), however, the influence of carbonates on the atmosphere in these regions has not yet been systematically studied. Investigation of the ion balance of November to May fresh snowfall at Arctic site Alert over a three year period (Toom-Sauntry and Barrie, 2002) led to the conclusion that missing carbonate (especially in November and May) is the most likely cause of the ion imbalance. In addition to dust, it is hypothesized

67   that a source of carbonates in summer Arctic aerosols may be marine microorganisms from sea spray as

68   reported by Mukherjee et al. (2020) based on calcium analyses.

69   In recent years, carbon in aerosols has also been subject to analyses of the stable isotopic composition ($\delta^{13}C$)

70   as a method for studying atmospheric processes (Gensch et al., 2014; Huang et al., 2006). Several studies

71   within the Arctic have also employed $\delta^{13}C$ analysis to study carbonaceous aerosols. Specifically, at the

72   Canadian Alert station, studies investigating $\delta^{13}C$ changes in the EC (Rodríguez et al., 2020; Winiger et al.,

73   2019) and springtime $\delta^{13}C$ changes in the TC (Narukawa et al., 2008) have recently been published.

74   Carbonates are strongly enriched in ^{13}C, with relatively positive $\delta^{13}C$ around zero, and can thus affect $\delta^{13}C$

75   values in TC of TSP aerosols, as demonstrated by Chen et al. (2016) for Asian desert dust. In the Arctic

76   region, observed higher aerosol $\delta^{13}C$ values in atmospheric aerosols are often attributed to dissolved

77   particulate organic matter from marine aerosol sources while the influence of carbonates is ignored (Gu et

78   al., 2023). We hypothesized that the influence of carbonates on Arctic aerosols is not negligible. In this

79   study, we present two years of carbonaceous aerosol observations at the Alert focusing on carbonate content

80   and the isotopic composition of $\delta^{13}C$ of TC.

81

82   **2 Experimental**

83   **2.1 Measurement site and sampling**

84   TSP samples were collected at the WMO Global Atmosphere Watch Observatory at Alert, Nunavut, Canada

85   (82°27'03.0" N, 62°30'26.0" W, 210 m ASL). The Alert site represents a remote Arctic area located on the

86   northeastern tip of Ellesmere Island, which is 817 km from the North Pole (**Fig. 1**). The site has been used

87   for research on atmospheric aerosols since the mid-1980s (Barrie and Barrie, 1990). In terms of

88   carbonaceous aerosols, BC has been measured at the station for decades (Sharma et al., 2004, 2017).

89   Rodríguez et al. (2020) later then reported EC/OC results from TSP between March 2014 to June 2015 with

90   a focus on EC analyses.

91   For this study, TSP samples were collected from June 13, 2016 to April 16, 2018, using a high-volume

92   sampler on pre-baked (450 °C, 12 h) quartz fiber filters (20 x 25 cm, PALL, 2500QAT-UP). During this

93   period, a total of 93 samples were collected at weekly intervals. The sampled filters were placed in clean

94   glass jars with Teflon-lined caps and stored in a freezer before chemical analyses.

95

Figure 1. Map of the site position (asterisk) and geographical boundaries for dominant source regions of backward air mass trajectories (Arctic Ocean - blue, Greenland - green, North Canada islands - red, North America - purple, Siberia - grey, and Europe - yellow). Background map by Wikimedia Commons / Public Domain.

2.2 Analyses

To obtain the TSP mass concentration, each filter was weighed before and after sampling, and resulting concentrations were corrected for the corresponding field blank filter. Subsequently, we analyzed the samples by two methods to measure the carbonaceous components, with the outputs shown in **Fig. 2**.

106
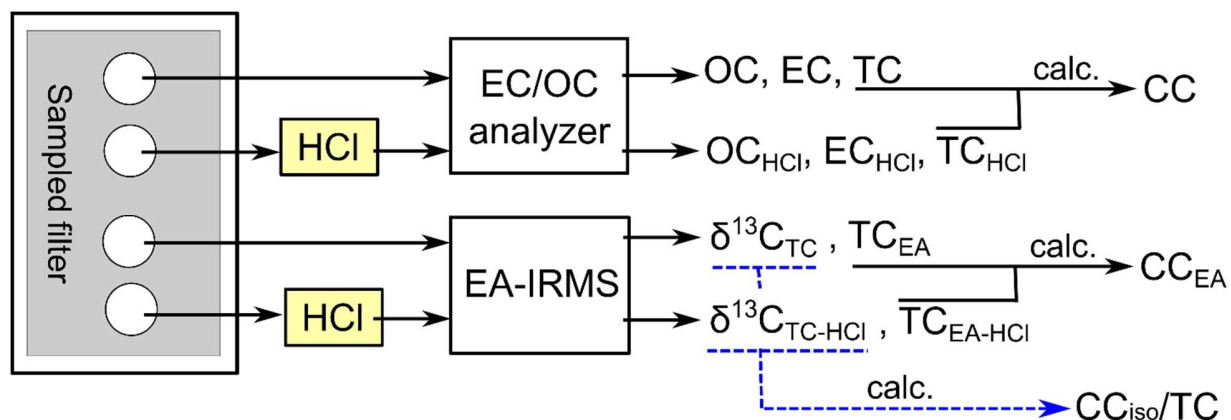
Figure 2. Diagram showing the method for the measurements of carbonaceous components in quartz fiber filter samples.

109

Contents of OC, EC and total carbon (TC) were determined using a Sunset semi-continuous analyzer (Sunset Laboratory Inc., Tigard, OR, USA; (Bauer et al., 2009)) operated in off-line mode. Samples with a diameter of 16 mm (area 2.01 cm^2) were analyzed by Improve_A temperature protocol: step [gas] temperature (°C)/duration (s): helium (He) 140/120, He 280/120, He 480/120, He 580/120, He-O2 (Ox.) 580/120, He-Ox. 740/120, He-Ox. 840/210 (Chow et al., 2007). Split point between OC and EC was determined based on laser beam (660 nm) transmittance measurements through the filter during analysis and raw data were subsequently evaluated by RTCalc726 software (Sunset Lab). The same EC/OC analysis was performed after exposing the aerosol filters to HCl vapors overnight in a desiccator. From the difference of TC and TC$_{HCl}$, the content of CC was calculated, which is discussed further in subsection 2.3.

The same samples were further analyzed for the stable carbon isotopic composition (δ^{13}C) of TC by the method described in more detail elsewhere (Vodička et al., 2022). Briefly, filter cuts (2.01 cm^2) were placed in tin cups, inserted into the elemental analyzer (EA, Flash 2000) and heated to 1000 °C in a helium atmosphere. At this temperature, carbonaceous compounds are evolved and catalytically oxidized to CO$_2$, which was isolated on a packed gas chromatograph, and then measured for TC by a thermal conductivity detector, and finally transferred into the isotope ratio mass spectrometer (IRMS; Delta V, Thermo Fischer Scientific) via a Conflo IV interface for the analyses of ^{13}C/^{12}C ratios. An external standard, acetanilide (supplied by Thermo Electron Corp.), having a δ^{13}C of −27.26 ‰ compared to Vienna Pee Dee Belemnite (VPDB), was used to obtain calibration curves for total carbon (TC) and its isotopic values. Subsequently, we determined the δ^{13}C of TC using **Eq. (1)** with relation to the international standard VPDB.

$$\delta^{13}C\ (‰) = [(^{13}C/^{12}C)_{sample} / (^{13}C/^{12}C)_{standard} − 1] \times 10^3 \qquad (1)$$

130   In this manner, $\delta^{13}C_{TC}$, corresponding to delta TC values on the filter, and $\delta^{13}C_{TC\text{-}HCl}$, representing delta

131   values on filters after exposure to HCl vapor, were analyzed. The standard deviation of $\delta^{13}C$ measurements

132   based on triplicate sample analysis was 0.03 ‰.

133   Through these analyses, we obtained TC from two independent analytical techniques. We observed good

134   agreement between TC value measured by the EC/OC analyzer and those by EA (r = 0.98). We also

135   obtained a good agreement even after HCl treatment of the filters (r = 0.98) (**Fig. S1**). The slightly higher

136   TC concentrations using EA (2 %) may be due to the use of a higher maximum temperature (1000 °C vs

137   840 °C) for sample release.

138

139   **2.3 Characteristics of carbonate carbon (CC)**

140   Concentrations of CC, one of the key variables of this study, were calculated from the difference of TC

141   before and after HCl fumigation (**Eq. (2)**)

142   $CC = TC - TC_{HCl}$ (2)

143   **Eq. (2)** defines CC, or nominal CC. This procedure is probably not able to analyze all carbonates (Baudin

144   et al., 2023) but quantitatively, this method leads to the analysis of at least 90% of the carbonates in samples

145   (Karanasiou et al., 2011). **Fig. 3** shows thermograms from OC-EC analyses of a selected sample without

146   HCl treatment (purple curve) and after HCl treatment (green curve). As shown in **Fig. 3**, the largest material

147   loss can be seen at the temperature step EC2, but for other samples we observed the largest material losses

148   in the EC1 and OC4 regions as well. These are temperature steps during which we should expect the release

149   of carbonate carbon (CC) (Cavalli et al., 2010; Chow et al., 1993). On the other hand, removal of carboxylic

150   acids (e.g. acetic or oxalic acid) can be expected at temperature steps OC2 and OC3 (Hasegawa, 2022).

151   Exposing samples to HCl can also affect the transformation of organic matter, which is then released at

152   higher temperatures. Therefore, the thermogram after fumigation may not reflect only the expected CC loss

153   (Jankowski et al., 2008). We also analyzed several carbonate and oxalate salt standards as a control (**Fig.

154   S2**). The thermogram of the sample with a pronounced peak in the EC2 region (**Fig. 3**) was most similar to

155   that of $CaCO_3$ (**Fig. S2a**). Hence, it can be assumed that the significant peaks, removed by HCl in the EC2

156   region of thermogram, are carbonate in origin. Nevertheless, it cannot be excluded that some of the

157   prominent CC peaks in the OC4 region are also from oxalates as confirmed also by additional analyses of

158   $CaCO_3$ and potassium oxalate monohydrate standards before and after HCl fumigation (**Fig. S2b**). The

159   nominal CC may contain other minor carbon components. Here, however, it should also be noted that the

160 reported values of oxalates in the Arctic (see, e.g., Feltracco et al. (2021), Svalbard) are an order of

161 magnitude lower than the CC values we analyzed.

162 It is worth noting here that if we did not analyze CC, it would be determined as either OC or EC based on

163 the thermogram and automatic determination of the split point (**Fig. 3**). For both EC and OC, we calculated

164 the percentage of mass removed by HCl fumes as CC using an **Eqs. (3)** and **(4)**.

165 $EC_{removed} (\%) = (EC - EC_{HCl})/EC *100$ (3)

166 $OC_{removed} (\%) = (OC - OC_{HCl})/OC *100$ (4)

167 In this way, we found that the CC contribution was, on average, 25 % (ranging from 0 to 81%) of EC and

168 12 % (ranging from 0 to 46 %) of OC which have been inaccurately determined if we had not assessed the

169 CC contribution. On a relative basis, EC concentrations were more biased in all seasons (**Fig. S3**).

170 Analyses for CC were performed by two independent methods (EC/OC and EA instruments, **Fig. 2**), and

171 the resulting CC values show acceptable agreement (**Fig. S4**). **Fig. S4** shows that CC values based on

172 analyses from the EC/OC analyzer may be slightly underestimated. However, unless otherwise stated, CC

173 values calculated from EC/OC analyses are discussed in this study.

174
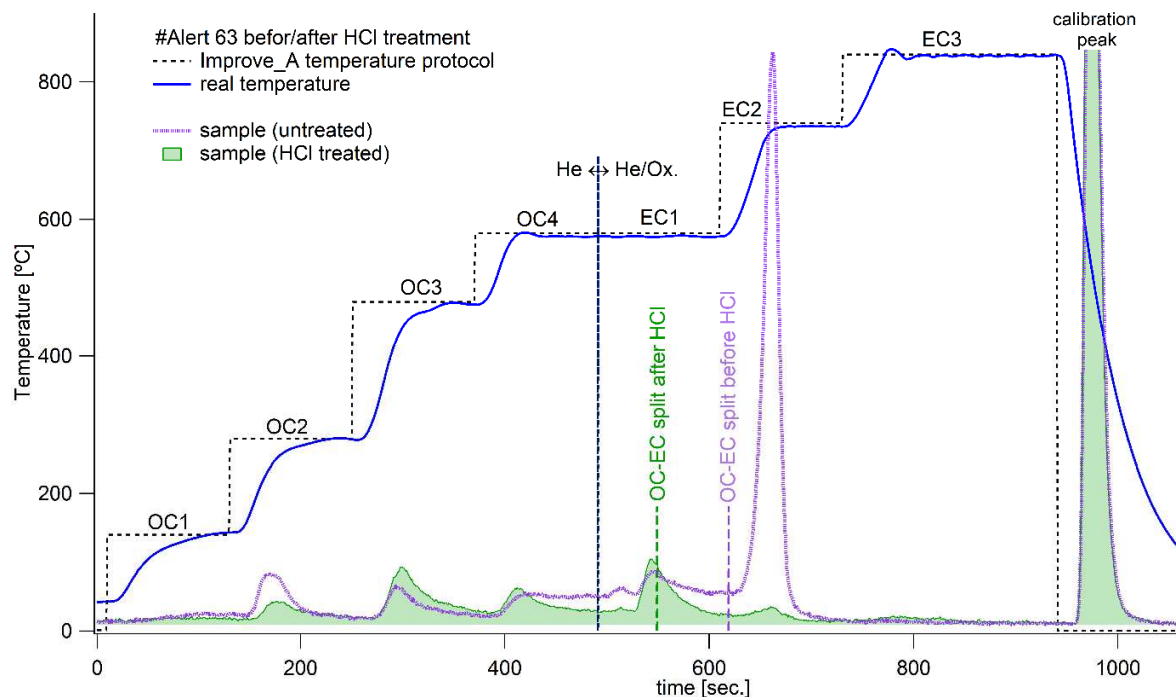
175 **Figure 3.** Example of EC/OC analysis of untreated (purple thermogram) and treated sample with HCl

176 fumigation (green thermogram) by Improve_A temperature protocol. The vertical black dashed line shows

177 a change in the use of He and the He/Ox. mixture in the analysis. The green and purple vertical dashed lines

178 show the automatic determination of split point between OC and EC. Sample #Alert-63 was collected from

179 15-22 May 2017.

180

181 **2.4 Estimate of $\delta^{13}C$ values of CC**

182 The $\delta^{13}C$ analyses of TC and TC_{HCl} allowed us to estimate $\delta^{13}C$ of CC. Here we calculate the $\delta^{13}C$ values

183 of released CC on HCl fumigation using the following reaction and the isotopic mass balance equation (**Eq.**

184 **5**), being similar with the calculation in Kawamura and Watanabe (2004).

185 $TC + HCl \rightarrow CO_2$ (carbonate carbon) $+ TC_{HCl}$
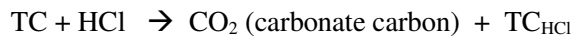
186 $\delta^{13}C_{TC} = f * \delta^{13}C_{CC} + (1\text{-}f) * \delta^{13}C_{TC\text{-}HCl}$ $\qquad$ (5)

187 , where f means a fraction of CC in TC. From **Eq. 5**, we derived the formula for calculating $\delta^{13}C_{CC}$ (**Eq. 6**).

188 $\delta^{13}C_{CC} = (\delta^{13}C_{TC} - (1\text{-}f) * \delta^{13}C_{TC\text{-}HCl}) / f$ $\qquad$ (6)

189 The $\delta^{13}C_{CC}$ values were reasonable for a CC content in the TC of approximately above 20 % (**Fig. S5**).

190 When f (CC contribution) is high, $\delta^{13}C_{CC}$ values are close to zero, supporting that CC is mainly composed

191 of carbonate, such as $CaCO_3$. However, when the f values are low, the $\delta^{13}C_{CC}$ are highly scattered, indicating

192 that the released (removed) carbon by HCl is not only carbonate carbon but also contains various types of

193 carbon including semi-volatile organic acids or unknown species. In the case of organic acids, $\delta^{13}C$ values

194 can be as high as $-10\,‰$ (e.g., Wang and Kawamura, 2006) or positive due to unknown isotope fractionation

195 during analytical processing. Highly scattered values may also be due to potential analytical errors in EA-

196 IRMS measurements when f is sufficiently small. If the CC contribution were zero, **Eq. 6** would lead to

197 division by zero. This may also be the cause of bias and scattering of $\delta^{13}C_{CC}$ values at low CC contributions

198 (**Fig. S5**).

199

200 **2.5 Carbonate estimation from isotopic composition**

201 We used the isotopic mass balance between $\delta^{13}C_{TC}$ and $\delta^{13}C_{TC\text{-}HCl}$ as an alternative and probably more

202 accurate method to determine carbonate content (CC_{iso}) in TC. The CC_{iso}/TC (f_{iso}) calculation is based on

203 the assumption that the $\delta^{13}C$ of carbonates is around 0 ‰ with an approximate range +5 ‰ to -5 ‰, and no

204 other compounds are present in this range. We used **Eq.5**, where $\delta^{13}C_{TC}$ and $\delta^{13}C_{TC\text{-}HCl}$ are known and $\delta^{13}C_{CC}$

205 are given by three different values, covering an approximate range of carbonates (+5 ‰, 0 ‰, -5 ‰).

206   While $\delta^{13}C_{CC} = 0$, $f = 1 - (\delta^{13}C_{TC} / \delta^{13}C_{TC\text{-}HCl})$ (7)

207   While $\delta^{13}C_{CC} = +5$, or -5, $f = (\delta^{13}C_{TC} - \delta^{13}C_{TC\text{-}HCl}) / (\delta^{13}C_{CC} - \delta^{13}C_{TC\text{-}HCl})$ (8)

208   The f_{iso} value is then an average calculated from the three f values obtained from **Eqs. 7** and **8**.

209

210   **2.6 Auxiliary data**

211   Air mass back trajectories (AMBT) were calculated using the National Oceanic and Atmospheric
212   Administration (NOAA) HYSPLIT model (Stein et al., 2015) at 500 m a.g.l. using a run time 168 h in
213   GDAS (Global Data Assimilation System) with 0.5 degree resolution for each sampling days. For
214   subsequent analyses, we divided the air masses into six sectors as depicted in **Fig 1**.

215   Meteorological data at 5 min resolution for temperature (T), wind speed (WS) and wind direction (WD)
216   were provided by Environment and Climate Change Canada. Only WDs between 14 November 2016 and
217   16 January 2017 were obtained from the NOAA website (https://psl.noaa.gov/arctic/observatories/alert/).
218   For the purpose of this study, complementary mean values of T and WS were calculated to each sample.

219   The WD and WS data were used to create wind roses by Zefir software (Petit et al., 2017) and used in
220   combination with the AMBT data to determine the predominant aerosol origin for each sample. All wind
221   roses and AMBT by HYSPLIT are shown in supplementary data.

222   The water soluble ions (Ca^{2+}, Mg^{2+}, Na^+) were measured using an ion chromatography (761 Compact IC,
223   Metrohm, Switzerland). For this purpose, the filtered samples were twice extracted with 10 ml of ultrapure
224   water using an ultrasonic bath for 15 min and the aqueous extracts were filtered using a disc filter (Millex-
225   GV, 0.22 µm, Millipore).

226

227   **3 Results and discussion**

228   **3.1 Carbonaceous aerosol composition**

229   Time series of TC, OC_{HCl}, EC_{HCl} and CC mass concentrations are shown in **Fig. 4**. An overview of results
230   is provided for the seasonal variations from 2016 to 2018 in **Table 1** and **Fig. S6** in supplementary material.
231   An average TC concentration over the entire measurement period was 0.219 ± 0.147 µg m^{-3} (median 0.186
232   µg m^{-3}; deviation due to one sample with a concentration of 1.22 µg m^{-3}, **Fig. 4a**). Average TC contribution
233   in aerosol mass ranged from 5 to 14% (**Table 1**). Seasonally, the highest mass concentrations of TC, OC_{HCl}
234   and EC_{HCl} were found in winter and/or spring (**Fig. S6**, **Table 1**).

235 The fact that EC_{HCl} corresponds to realistic elemental carbon concentrations is demonstrated by comparison
236 with the study of Rodríguez et al. (2020), who analyzed EC in TSP during 2014-2015. They reported
237 seasonal EC concentrations that are similar to our observed EC_{HCl}, while their CC was part of the OC due
238 to the use of a different temperature protocol (EnCan-Total-900) during the OC/EC analysis. However,
239 Rodríguez et al. (2020) did not quantify the contribution of CC to TC.

240 Concentrations of OC_{HCl} dominate in all seasons (**Figs. 4b** and **5**) but present seasonally different
241 correlations with ambient temperature. Especially in summer, we observe a significant positive correlation
242 (r = 0.73) between OC_{HCl} concentrations and temperature (**Fig. S7a**). A similar relationship was also
243 observed, e.g., at the subarctic station Pallas (Friman et al., 2023), suggesting a biogenic origin of
244 summertime organic aerosols in Arctic areas (Moschos et al., 2022). In contrast, we observe negative
245 correlations between OC_{HCl} and ambient temperature in winter (r = -0.15, insignificant) and spring (r = -
246 0.43). A year-round similar trend for EC_{HCl} (r = -0.39, **Fig. S7b**), supporting previous studies that highlight,
247 in particular, the anthropogenic contributions to Arctic aerosol during the polar night (Moschos et al., 2022).
248 However, for CC, we observe no significant dependence on temperature (r = 0.09, **Fig. S7c**).

249
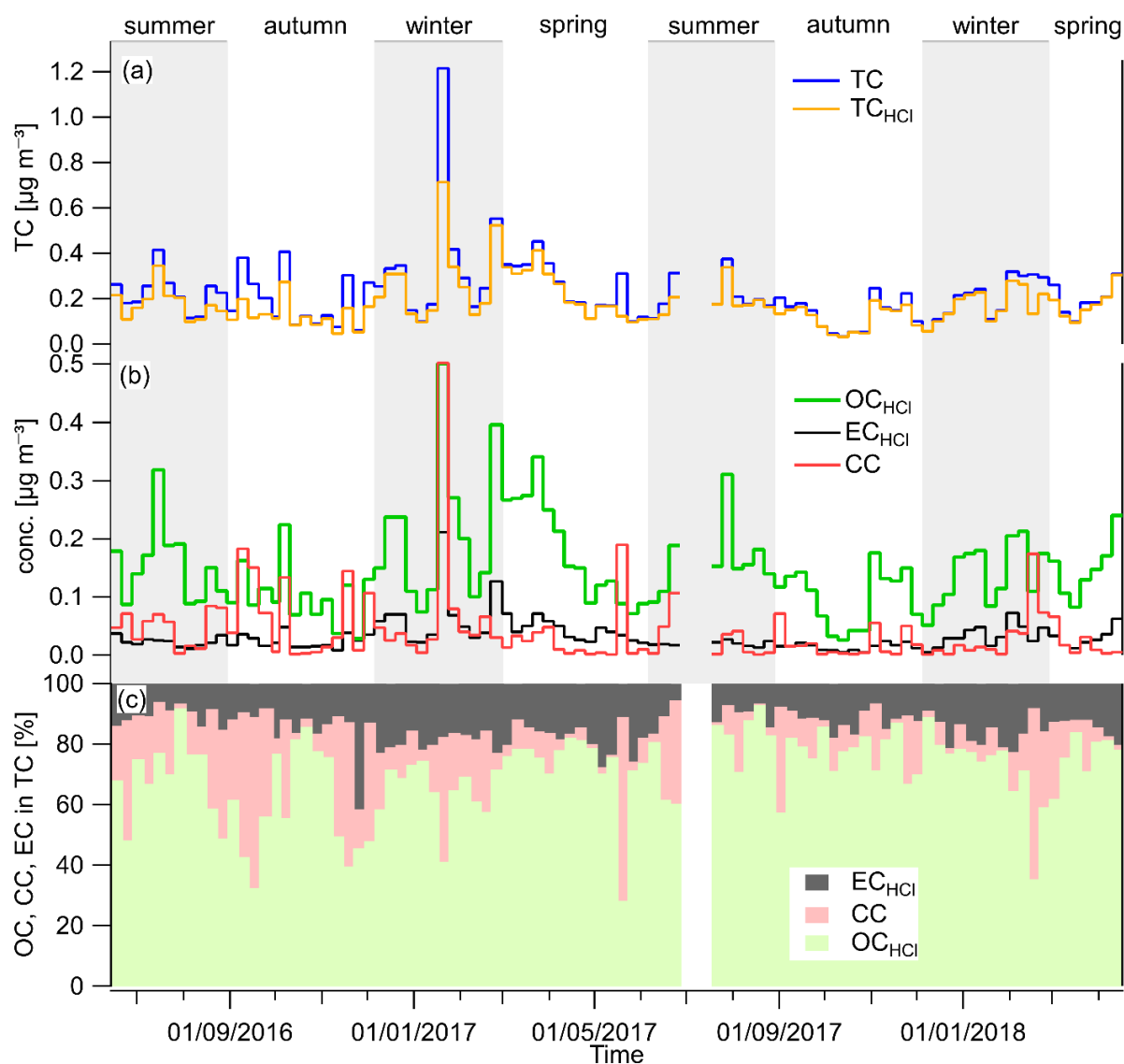
Figure 4. Time series of (a) TC mass concentrations before and after HCl treatment of samples, (b) OC, EC and CC mass concentrations, and (c) their relative contributions to TC in the Alert TSP aerosols.

Time series of TC before and after HCl fumigation (**Fig. 4a**) show that the amount of carbon removed in the form of CC is neither negligible nor large. However, both mass concentrations of CC (**Fig. 4b**) and its relative contributions (**Fig. 4c**) show that the CC is often larger than the EC_{HCl} contribution. Specifically, CC concentrations were highest during both autumn of 2016 and summer of 2016 and 2017 (**Fig. S6c**), which was reflected also in the relative contributions to TC (**Table1, Fig. 5**).

259 It is notable to understand the origin of CC. During summer, the contribution of biogenic aerosols (a
260 potential source of oxalates) is highest, while the landscape is least covered by snow, making the situation
261 favorable for resuspension of soils eroded from rocks including carbonates. A potential source of carbonates
262 may come directly from the Canadian Arctic land region, where limestone sediments are reported to be
263 abundantly present (Groot Zwaaftink et al., 2016; Not and Hillaire-Marcel, 2012; Phillips and Grantz, 2001).
264 Another likely source of carbonate is marine aerosols as marine organisms contribute carbonate to the sea
265 (Stein et al., 1994). In the context of wind directions and the effect on $\delta^{13}C$, the origin of CC is further
266 discussed in the following subsection 3.2.
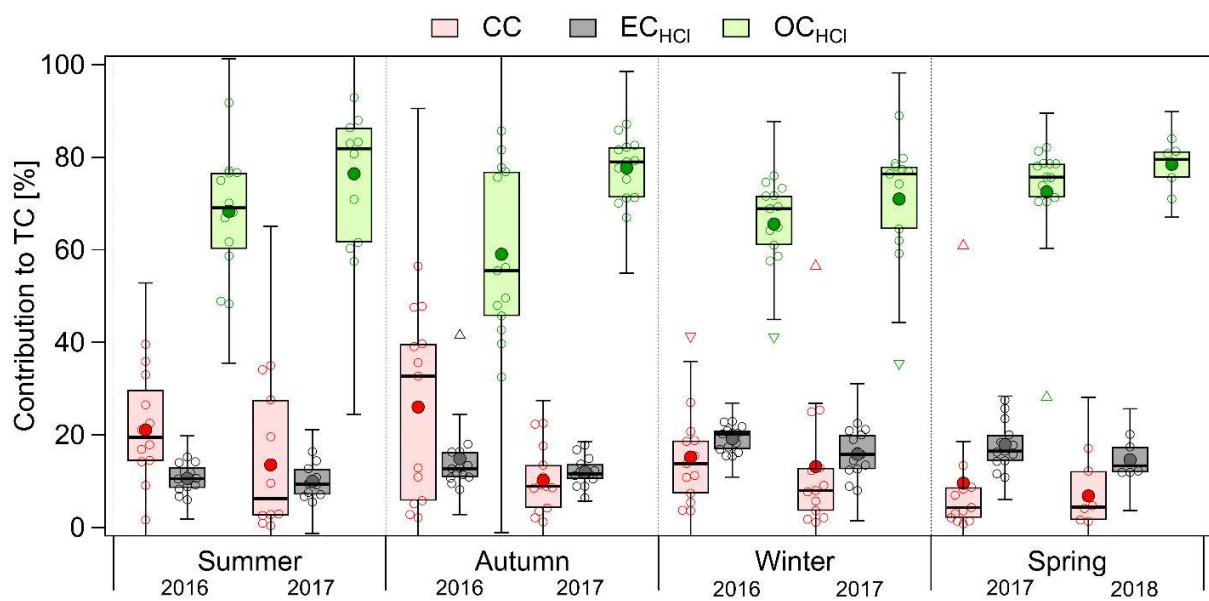
268 **Figure 5.** Seasonal contributions of CC, EC_{HCl} and OC_{HCl} to TC. The boxes correspond to the interquartile
269 range (IQR; 25 and 75 percentile) with median represented by the inner solid line. The whiskers correspond
270 to inner fences range (1.5*IQR), triangles are outliers and mean is represented by large filled circle.

271

3.2. Stable carbon isotopic composition

273 Removal of CC by HCl fumigation has a significant effect on the measurements of $\delta^{13}C$ isotopic values of
274 TC (**Figs. 6** and **7**). **Fig. 6** shows a seasonally resolved $\delta^{13}C$ values for HCl-treated (red) and untreated
275 (grey) samples. We observed significant changes in all seasons except in spring of 2017 and 2018. Here it
276 is interesting to mention a link with Narukawa et al. (2008), who reported changes in $\delta^{13}C$ of TC values for
277 HCl-treated samples between winter and spring at Alert site. Narukawa et al. (2008) show significantly
278 higher $\delta^{13}C$ values in spring than winter and related this to the possible contribution of carboxylic acids

279 (especially oxalic acid). During our observations, the differences in average values of $\delta^{13}C$ of TC (HCl

280 treated vs. untreated) were also significant (see red boxes in **Fig. 6** and **Table 1**). Winter and spring $\delta^{13}C$

281 values after HCl treatment in this study (**Table 1**) are similar to those presented by Narukawa et al. (2008)

282 for the year 2000. Thus, this study confirms that this is a long-term phenomenon likely to occur annually.

283

284
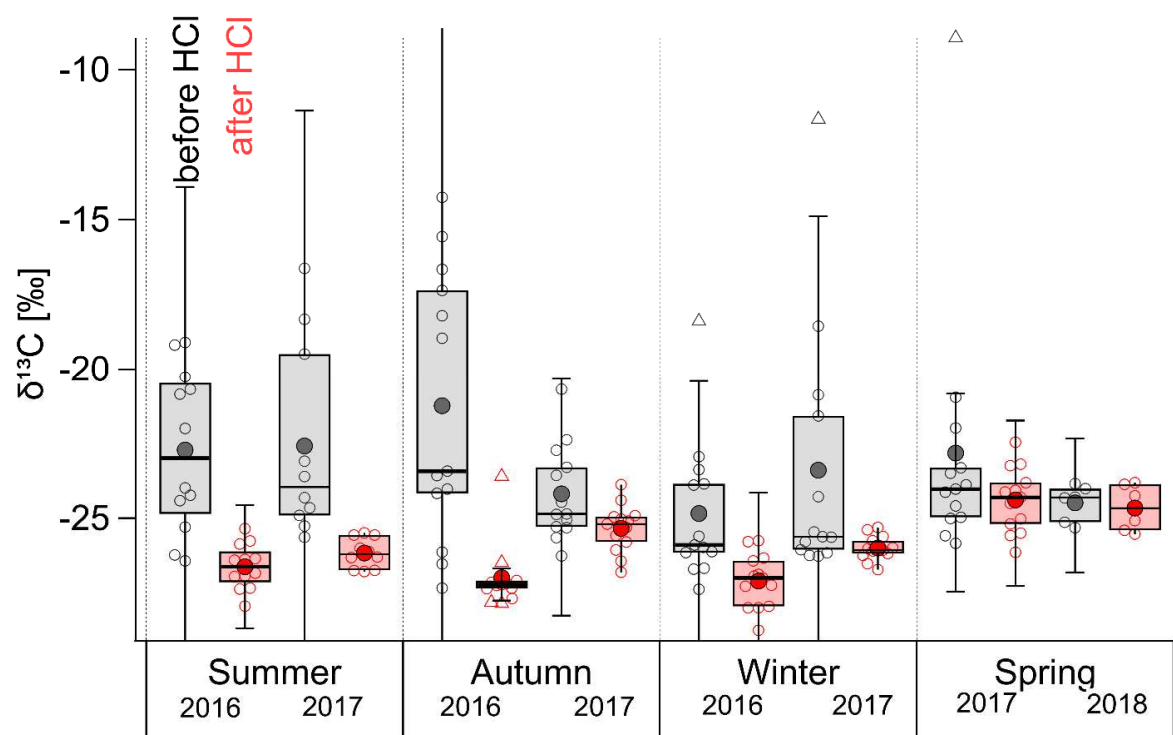
285 **Figure 6.** Seasonal variations of $\delta^{13}C$ of TC of untreated (grey) and HCl treated (red) TSP samples at Alert

286 site from summer 2016 to spring 2018. The boxes correspond to the interquartile range (IQR; 25 and 75

287 percentile) with median represented by the inner solid line. The whiskers correspond to inner fences range

288 (1.5*IQR), triangles are outliers and mean is represented by large filled circle.

289

290 In addition, measurements of $\delta^{13}C$ in OC, pyrolytic carbon (POC) + CC, and EC, performed at Environment

291 Canada Toronto Laboratory, using ECT9 temperature protocol (Huang et al., 2006, 2021) for the fine

292 particle (PM_1) samples collected around 2003, support that a noticeable fraction of CC occurs during the

293 summer months, as indicated by the relatively more positive $\delta^{13}C$ of "POC+CC" fraction (**Fig. S8**).

294 Carbonate from eroded rocks in terrestrial environment usually generates large particles, so the CC content

295 in PM_1 should be lower than that in TSP. Consequently, the $\delta^{13}C$ TC in PM_1 is expected to be relatively

296 less positive of compared to that that in TSP. Therefore, **Fig. S8** suggests that the impact of CC on $\delta^{13}C$ TC

297 is an annual phenomenon occurring over decadal periods. The tendency towards relatively more positive

298 $\delta^{13}C$ in summer OC fraction also suggests the presence of minor salt oxalate, or potassium or magnesium

299 carbonates, which are released at 550 °C or lower, as shown in **Fig. S2**. In the time series in **Fig. 7**, we

300 observed episodes with significant differences in $\delta^{13}C$ values and alternating over short periods. The

301 comparison of $\delta^{13}C$ of TC and TC mass concentration for both HCl untreated and treated samples shows

302 insignificant correlation (**Fig. S9**). However, we found a significant, though not strong, correlation of $\delta^{13}C$

303 with wind speed (**Fig. S10**) (r = 0.36) and a negative correlation after HCl fumigation (r = -0.32 for $\delta^{13}C_{TC\text{-}HCl}$

304 vs. wind speed). Concentrations of CC were also positively correlated with wind speed (r = 0.48, **Fig.**

305 **S10**), indicating that wind has an effect on this aerosol component. Therefore, we compared the $\delta^{13}C$ time

306 series with average wind speeds and prevailing AMBT from the HYSPLIT model (see colored bars in **Fig.**

307 **7**), which were divided into six regions as shown in **Fig. 1.**

308 The large differences in $\delta^{13}C$ values (or relatively more positive $\delta^{13}C_{TC}$ values) can be divided into three

309 categories. The most frequent differences were observed during periods of stronger winds (average WS

310 above 4 m s^{-1}) associated with the prevailing back trajectories from the North Canada region. These episodes

311 can be found mainly in summer and autumn 2016 and summer 2017. Such conditions favor dust

312 resuspension, which may also contain limestone, known to be abundant in this region (Not and Hillaire-

313 Marcel, 2012; Phillips and Grantz, 2001). The presence of a peak in soil dust carbonates in late

314 summer/early autumn is consistent with multidecadal aerosol aluminum observations at Alert (Sharma et

315 al., 2019; Sirois and Barrie, 1999). These observations also indicate a peak in soil dust aerosol in the spring

316 month of May (Sharma et al. 2019).

317 Second, in late February/March 2018, we observed significant enrichment of ^{13}C, which may probably be

318 linked to long range transport (LRT) from/over Europe, Greenland and North America (Fig. 6). Sources of

319 carbonate in this case may be, for example, calcifying marine phytoplankton (Monteiro et al., 2016), which

320 are abundant in the North Atlantic (Okada and Honjo, 1973). Another possibility is the volcanic and

321 subarctic semi-desert areas in Iceland (Arnalds et al., 2016).

322
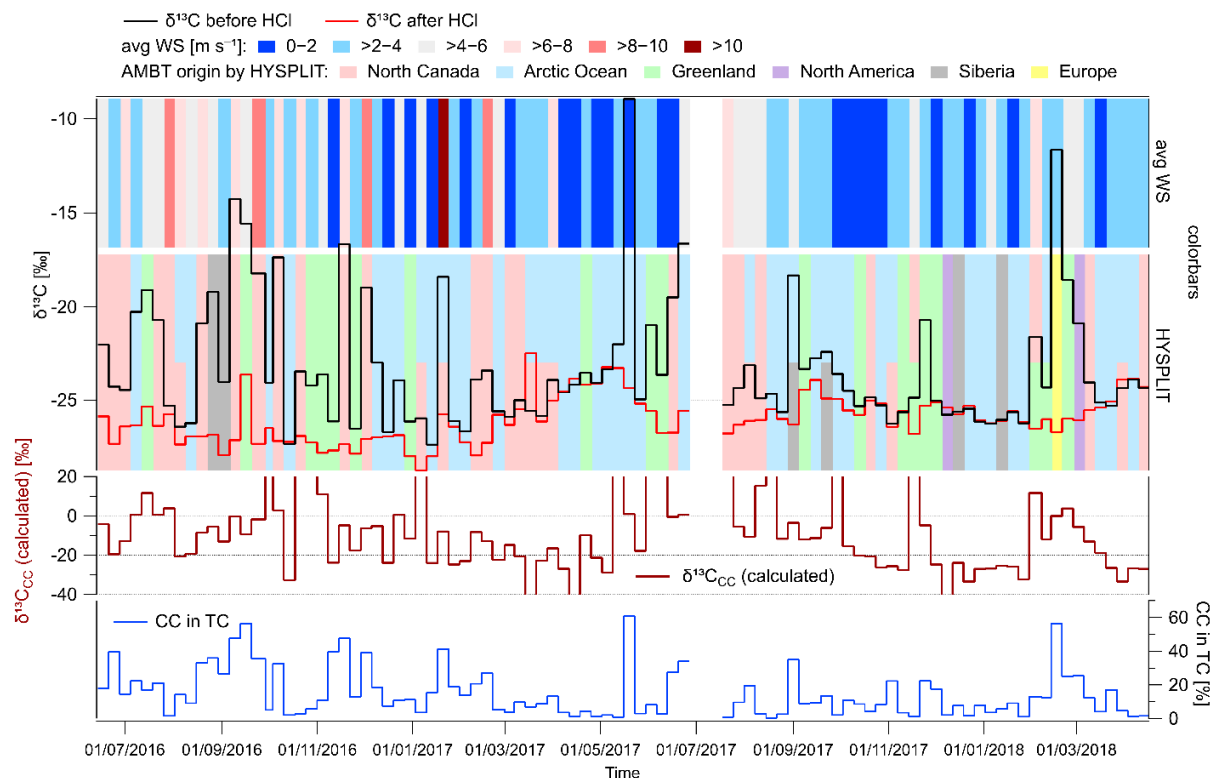
Figure 7. Time series of isotopic composition (δ^{13}C) of TC before and after HCl treatment of samples (upper part) with color bars representing average wind speed (top) and origin of AMBT based on HYSPLIT model and divided to regions shown in Fig. 1 (middle part). Time series of the calculated $\delta^{13}C_{CC}$ (outliers less than -40 ‰ and more than +20 ‰ not depicted) and contribution of CC in TC (bottom).

The third case is a δ^{13}C difference observed during lower wind speeds coming from the Arctic Ocean or Greenland. This includes also the sample taken between 15-22 May 2017, whose thermograms are shown in **Fig. 3**, and which was most enriched in ^{13}C carbon. A recent study by Gu et al. (2023), which reports observations of summer carbonaceous aerosols in the Arctic Ocean, is relevant in this context. They also observed relatively more negative δ^{13}C values of TC, but in this case they did not consider the enriched ^{13}C carbon as a carbonate contribution, instead, they associated it with an input of fresh marine particulate organic carbon (MPOC) (Verwega et al., 2021). MPOC is formed by the conversion of inorganic carbon by marine phytoplankton through photosynthesis in ocean surface layer (Descolas-Gros and Fontugne, 1990), and this carbon can be partially released into the atmosphere as marine aerosol (Ceburnis et al., 2016). We cannot exclude the influence of MPOC on the TSP taken at the Alert station, but the specific EC/OC thermogram (**Fig. 3, Fig. S2**) shows rather an influence of CaCO₃. The presence of carbonates in surface seawater and their interference with organic coatings has been known for decades (Chave, 1965).

341 Dissolved CO_2 in the oceans consists mainly of inorganic substances, which are bicarbonates (HCO_3^-;

342 >85%) and carbonates (ca 10%), and their content varies with temperature, pH, salinity and other

343 parameters (Zeebe, 2012). Carbonate, in the form of $CaCO_3$, is generally supersaturated in surface seawater

344 but its precipitation may be limited due to dissolved organic matter (Chave and Suess, 1970). In addition

345 to common inorganic reactions due to dissolved CO_2, the carbonate cycle is also influenced by marine life.

346 Phytoplankton such as coccolithophores (e.g. *Emiliania huxleyi*), could also contribute to formation of

347 carbonates (Smith et al., 2012). These organisms produce calcified shells called coccoliths, which are about

348 2–25 μm across (Monteiro et al., 2016). While these microfossils are mostly deposited on the seabed, they

349 are also likely to be released also into the atmosphere with marine aerosol from the upper sea layers. Such

350 potential introduction of coccolith fragments by sea spray aerosol to the atmosphere is reported by

351 Mukherjee et al. (2020) for Arctic summer. Whether through MPOC or inorganic carbon, this

352 phytoplankton influences the fractionation of ^{13}C carbon (Holtz et al., 2017).

353 Coccolith microfossils contain enriched calcite with $\delta^{13}C$ values around 0 ‰ (McClelland et al., 2017).

354 Limestone sediments in the Canadian Arctic are even more enriched, with $\delta^{13}C$ values ranging from 2 to

355 8 ‰ (Beauchamp et al., 1987). After estimating $\delta^{13}C_{CC}$ (see subsection 2.4), we observed that with a high

356 CC abundance in TC, the calculated $\delta^{13}C_{CC}$ values are also seen around 0 ‰ (**Fig. 7** bottom, **Fig. S5**). This

357 suggests that when the TC contains a larger contribution of CC (suppose above 20%), it can be assumed

358 that a significant portion of the nominal CC is derived from limestone. However, the uncertainties in the

359 determining of $\delta^{13}C_{CC}$, mentioned in section 2.4, primarily due to the low CC contributions in TC, likely

360 prevent distinguishing whether the carbonates are from sediment resuspension or marine calcified shells.

361 Some insight, however, can be obtained from the AMBT analysis discussed earlier.

362 Finally, **Fig. 8a** confirms a strong dependence of $\delta^{13}C_{TC}$ on the CC content in TC (r = 0.79). The dependence

363 of $\delta^{13}C_{TC}$ directly on CC mass concentration is even stronger (r = 0.85, after excluding 1 outlier, **Fig. S11**).

364 Furthermore, we calculated the fractions of CC for individual samples via isotope mass balance (using a

365 $\delta^{13}C$ of CC value of zero as the end member, see subsection 2.5.) and found that, overall, the calculated

366 results were approximately 5 % lower than the measured CC/TC, with less scatter. In addition, we observed

367 an excellent correlation between $\delta^{13}C$ of TC and the calculated fraction of CC, with r = 0.96 shown in **Fig.**

368 **8b**, indicating that more than 92 % of the variation in $\delta^{13}C$ of TC can be explained by the dependency on

369 the fraction of CC.

370
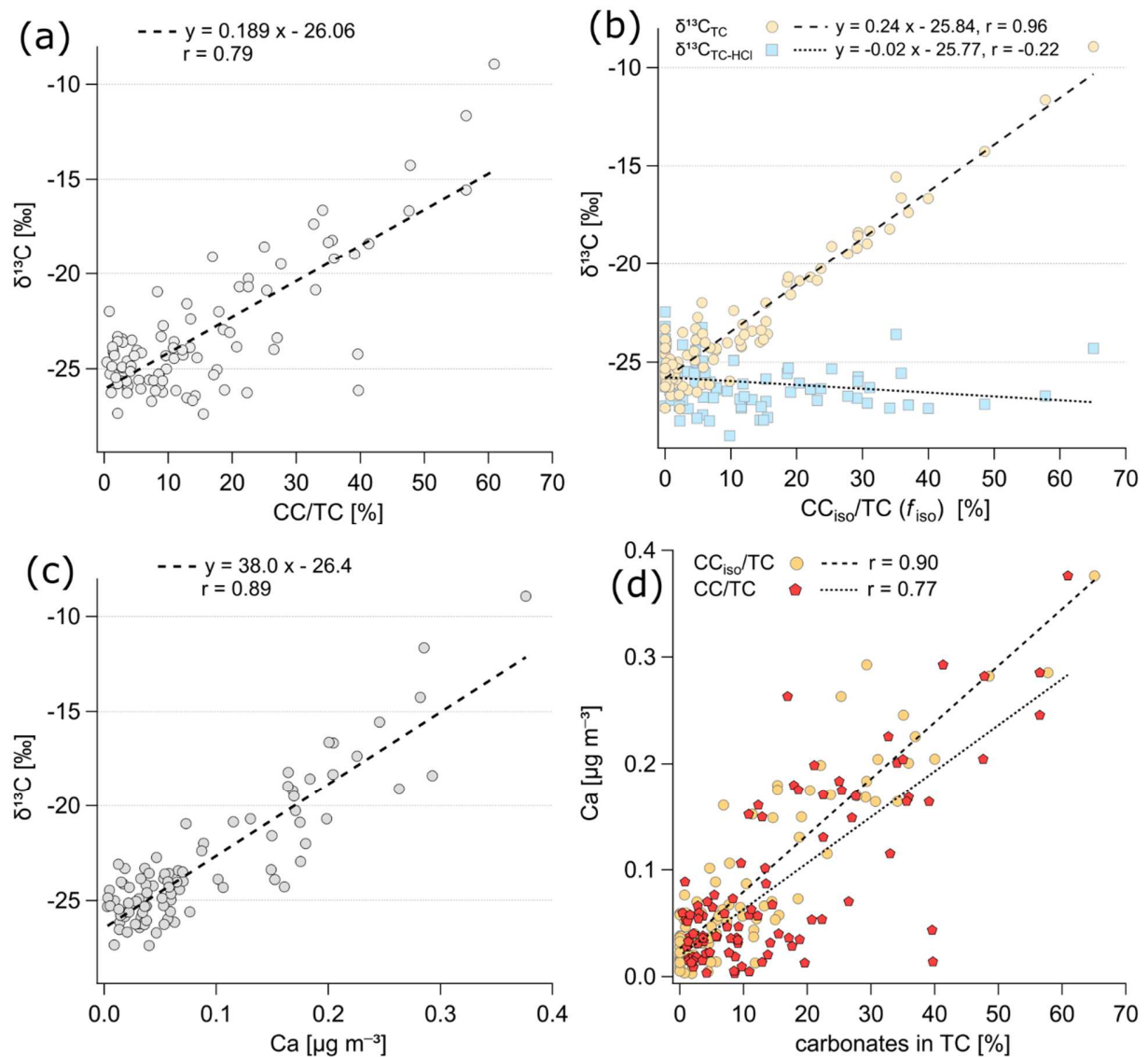
Figure 8. Dependence of (a) $\delta^{13}C_{TC}$ on the percentage contribution of CC in TC, (b) $\delta^{13}C_{TC}$ and $\delta^{13}C_{TC\text{-}HCl}$ on the calculated fraction of CC_{iso} in TC, (c) $\delta^{13}C_{TC}$ on Ca mass concentrations, and (d) Ca mass concentrations on percentage contribution of CC and CC_{iso} in TC.

Further support for the influence of $\delta^{13}C$ of TC in favor of carbonates is provided by its strong correlation with calcium (r = 0.89, **Fig. 8c**). Calcium is also strongly correlated with CC contribution in TC, with r = 0.90 for Ca vs. CC_{iso}/TC (**Fig. 8d**). Apportionment of Ca amongst aerosol sources at Alert site (Sharma et al., 2019), using multidecadal observations and Positive Matrix Factorization analyses, showed that, on

380   average for both the period November to February, and March to May, Ca was associated 84 and 85% with

381   windblown dust/soil and 12 and 8 % with sea salt aerosol, respectively.

382   We also investigated the possible contribution of carbon from magnesium carbonate. Magnesium was

383   strongly correlated with sodium (r = 0.91, **Fig. S12**), indicating its link mainly to marine aerosol. In contrast,

384   we observed no relationship between Mg and Ca; this dependence was strongly scattered (**Fig. S12**). Overall,

385   the results indicate that the main contribution of CC, that strongly influences the δ^{13}C of TC, is mainly

386    $CaCO_3$. If there is a contribution of magnesium carbonate, it is rather episodic.

387   These results thus provide evidence that the CC content in aerosols, mostly of soil origin and to a lesser

388   extent marine origin, strongly influences the δ^{13}C isotopic composition of TC in the Arctic atmosphere.

389   Further research at different Arctic sites could reveal whether the non-negligible presence of CC in the TSP

390   is the case only in the northern Canada region or a phenomenon observe in larger parts of Arctic.

391

4 Summary and conclusions

393   We found that the aerosol CC (i.e. carbonate carbon) fraction in Arctic TSP at Alert site is not negligible.

394   The relative abundances of CC in TC ranged from 0 to 60 % with an average of 11 % over the entire

395   measurement period. On average, 25 % (range: 0 to 81 %) of EC and 12% (range: 0 to 46 %) of OC was

396   identified here as nominal CC. The influence of CC removal from the sample was also significantly

397   reflected in the isotopic composition of δ^{13}C of TC. The effect of CC on δ^{13}C was particularly pronounced

398   in the summer of 2016 and 2017, as well as during autumn 2016 due to strong local Arctic dust transport.

399   In contrast, the effect of removing of CC on δ^{13}C was lowest in spring. Thus, CC content in TSP at Alert

400   can sometimes strongly influence the δ^{13}C values of aerosols.

401

402   Based on the thermograms from EC/OC analyses and the calculated $\delta^{13}C_{CC}$, whose values were around 0

403   ‰ at high CC contributions to TC, we conclude that the major part of CC is derived from carbonates.

404   Additionally, based on the isotope mass balance calculation (using 0 ‰ as $\delta^{13}C_{CC}$), an excellent dependency

405   between δ^{13}C of TC and the calculated fraction of CC (r = 0.96) is observed, supporting that most of the

406   variation of δ^{13}C of TC were due to the contribution of CC. Based on the AMBT analyses, we identified

407   two possible carbonate sources. The first is eroded and resuspended limestone sediments in the northern

408   Canadian region. The second source may be calcareous shells (coccoliths) produced by marine

409   phytoplankton and transported from both the Arctic Ocean and the North Atlantic Ocean. However, the

410   hypothesis of these sources requires further detailed research.

411

412   In general, when analysing $\delta^{13}C$ of TC in coarse aerosol or aerosols laden with dust, it must be taken into
413   account that the resulting values may be strongly influenced by CC content. If CC is not removed prior to
414   EC/OC analysis, CC may be mistakenly identified as EC during Improve_A analysis. This could, for
415   example, affect modelling of the effect of carbonaceous aerosols on the Arctic climate, as EC (or black
416   carbon) has a warming effect on the atmosphere, while CC has a lower warming effect.

417

418   **Data availability.** All relevant data for this paper are archived and are available upon request from the
419   corresponding authors or online at repository here: https://zenodo.org/records/14204515

420

421   **Supplementary data**
422   Supplementary data to this article can be found as a pdf file uploaded together with this manuscript.

423

424   **Author contribution.** All authors contributed to the final version of this article. PV analyzed EC/OC
425   before and after HCl treatment, as well as $\delta^{13}C$ of TC, AMBT analyses, evaluated all data and wrote the
426   paper under the supervision of KK. BK analyzed $\delta^{13}C$ of TC after HCl treatment as well as supporting water
427   soluble ions measurements. LH calculated contribution of CC_{iso}/TC based on $\delta^{13}C$ measurements. DD and
428   MMH assisted in the gravimetry and other sample treatments. AP was responsible for the evaluation of Ca,
429   Mg and Na data. SS provided meteorological data. SS with KK and LB managed the field campaign. All
430   authors provided advice and feedback throughout the drafting and submission process.

431

432   **Competing interests.** Kimitaka Kawamura is an editor for Atmospheric Chemistry and Physics. The
433   authors declare that they have no other conflict of interest.

434

440

441

442

Table 1: Seasonal averages ± standard deviations (medians in parentheses) of different variables in TSP at Alert site.

	Summer 2016	Autumn 2016	Winter 2016	Spring 2017	Summer 2017	Autumn 2017	Winter 2017	Spring 2018
N	12	13	13	13	10	13	13	6
OC [μg m^{-3}]	0.182±0.075 (0.177)	0.136±0.072 (0.106)	0.253±0.171 (0.237)	0.184±0.092 (0.151)	0.179±0.071 (0.155)	0.106±0.06 (0.128)	0.154±0.057 (0.177)	0.154±0.053 (0.153)
EC [μg m^{-3}]	0.037±0.021 (0.032)	0.056±0.055 (0.023)	0.100±0.121 (0.070)	0.057±0.037 (0.047)	0.031±0.015 (0.026)	0.019±0.013 (0.017)	0.055±0.036 (0.046)	0.032±0.018 (0.029)
TC [μg m^{-3}]	0.219±0.082 (0.216)	0.193±0.120 (0.126)	0.353±0.287 (0.290)	0.240±0.113 (0.186)	0.210±0.076 (0.186)	0.125±0.070 (0.146)	0.209±0.088 (0.225)	0.186±0.071 (0.182)
OC$_{HCl}$ [μg m^{-3}]	0.150±0.067 (0.144)	0.103±0.052 (0.095)	0.215±0.125 (0.201)	0.172±0.088 (0.149)	0.159±0.062 (0.150)	0.096±0.051 (0.111)	0.140±0.052 (0.161)	0.146±0.056 (0.138)
EC$_{HCl}$ [μg m^{-3}]	0.022±0.008 (0.022)	0.024±0.012 (0.021)	0.067±0.052 (0.058)	0.040±0.015 (0.040)	0.019±0.004 (0.019)	0.014±0.007 (0.015)	0.034±0.018 (0.031)	0.029±0.018 (0.024)
TC$_{HCl}$ [μg m^{-3}]	0.172±0.070 (0.165)	0.127±0.061 (0.115)	0.282±0.175 (0.250)	0.211±0.101 (0.175)	0.178±0.064 (0.169)	0.110±0.057 (0.128)	0.174±0.068 (0.194)	0.175±0.074 (0.162)
CC [μg m^{-3}]	0.047±0.028 (0.052)	0.066±0.068 (0.030)	0.071±0.131 (0.034)	0.029±0.051 (0.010)	0.032±0.036 (0.020)	0.015±0.018 (0.006)	0.035±0.048 (0.014)	0.011±0.011 (0.007)
TC/mass [%]	10.3±3.8 (9.4)	6.0±1.9 (5.9)	7.8±3.5 (8.3)	5.9±2.4 (5.4)	13.2±5.4 (13.7)	8.3±6.2 (7.3)	6.0±1.6 (5.2)	7.8±1.8 (7.3)
CC/TC [%]	21.1±11.2 (19.5)	26.1±19.8 (32.7)	15.2±10.6 (13.8)	9.6±15.9 (4.3)	13.5±14.2 (6.2)	10.2±7.1 (8.9)	13.2±15.2 (8.0)	6.8±6.4 (4.4)
CC$_{iso}$/TC [%]	15.0±9.6 (14.9)	22.0±16.0 (15.6)	8.5±8.5 (6.7)	7.8±17.9 (1.2)	14.2±12.6 (9.8)	4.6±5.3 (4.4)	10.3±17.4 (0.2)	1.2±2.4 (0.0)
OC$_{HCl}$/TC [%]	68.3±12.5 (69.1)	59.0±18.1 (55.5)	65.6±9.5 (68.9)	72.5±13.9 (75.7)	76.5±12.8 (81.8)	77.7±6.3 (79.0)	71.0±13.4 (76.4)	78.5±4.6 (79.5)
EC$_{HCl}$/TC [%]	10.6±3.0 (10.5)	14.9±8.5 (12.7)	19.2±2.7 (20.2)	17.9±5.1 (16.5)	10.0±3.6 (9.3)	12.0±3.2 (11.6)	15.8±4.7 (15.8)	14.7±3.4 (13.3)
TC$_{EA}$ [μg m^{-3}]	0.218±0.101 (0.214)	0.184±0.118 (0.120)	0.345±0.263 (0.287)	0.234±0.119 (0.200)	0.199±0.079 (0.174)	0.126±0.067 (0.124)	0.227±0.100 (0.224)	0.195±0.083 (0.191)
δ^{13}C$_{TC}$ [‰]	-22.7±2.7 (-23.0)	-21.2±4.5 (-23.4)	-24.8±2.4 (-25.9)	-22.8±4.4 (-24.0)	-22.6±3.2 (-24.0)	-24.2±1.6 (-24.9)	-23.4±4.3 (-25.6)	-24.5±0.6 (-24.3)
TC$_{EA-HCl}$ [μg m^{-3}]	0.141±0.063 (0.136)	0.092±0.052 (0.079)	0.273±0.196 (0.253)	0.199±0.108 (0.169)	0.157±0.065 (0.144)	0.103±0.052 (0.099)	0.173±0.068 (0.188)	0.184±0.080 (0.166)
δ^{13}C$_{TC-HCl}$ [‰]	-26.6±0.7 (-26.6)	-27.0±1.1 (-27.2)	-27.1±0.9 (-27.0)	-24.4±1.1 (-24.3)	-26.2±0.5 (-26.2)	-25.3±0.8 (-25.2)	-26.0±0.4 (-26.1)	-24.7±0.8 (-24.7)
WS [m s^{-1}]	5.1±1.8 (4.5)	5.5±2.7 (5.6)	3.9±2.7 (3.1)	3.0±1.4 (3.5)	4.2±1.8 (4.6)	2.5±1.2 (2.1)	3.6±1.8 (3.4)	2.7±0.6 (2.6)
Temp. [°C]	5.0±4.6 (4.2)	-13.8±6.9 (-14.0)	-28.7±4.0 (-27.6)	-20.5±8.4 (-21.3)	1.2±4.6 (1.5)	-18.6±6.8 (-19.6)	-26.2±3.9 (-25.5)	-30.0±3.5 (-30.8)

445

References:

Arnalds, O., Dagsson-Waldhauserova, P. and Olafsson, H.: The Icelandic volcanic aeolian environment: Processes and impacts - A review, Aeolian Res., 20, 176–195, doi:10.1016/j.aeolia.2016.01.004, 2016.

Barrie, L. A. and Barrie, M. J.: Chemical components of lower tropospheric aerosols in the high Arctic: Six years of observations, J. Atmos. Chem., 11(3), 211–226, doi:10.1007/BF00118349, 1990.

Baudin, F., Bouton, N., Wattripont, A. and Carrier, X.: Carbonates thermal decomposition kinetics and their implications in using Rock-Eval® analysis for carbonates identification and quantification, Sci. Technol. Energy Transit., 78, doi:10.2516/stet/2023038, 2023.

Bauer, J. J., Yu, X.-Y., Cary, R., Laulainen, N. and Berkowitz, C.: Characterization of the sunset semi-continuous carbon aerosol analyzer., J. Air Waste Manag. Assoc., 59(7), 826–833, doi:10.3155/1047-3289.59.7.826, 2009.

Beauchamp, B., Oldershaw, A. E. and Krouse, H. R.: Upper carboniferous to upper permian 13C-enriched primary carbonates in the sverdrup basin, Canadian arctic: Comparisons to coeval Western North American Ocean Margins, Chem. Geol. Isot. Geosci. Sect., 65(3–4), 391–413, doi:10.1016/0168-9622(87)90016-9, 1987.

Carslaw, K. S., Lee, L. A., Reddington, C. L., Pringle, K. J., Rap, A., Forster, P. M., Mann, G. W., Spracklen, D. V., Woodhouse, M. T., Regayre, L. A. and Pierce, J. R.: Large contribution of natural aerosols to uncertainty in indirect forcing, Nature, 503(7474), 67–71, doi:10.1038/nature12674, 2013.

Cavalli, F., Viana, M., Yttri, K. E., Genberg, J. and Putaud, J.-P.: Toward a standardised thermal-optical protocol for measuring atmospheric organic and elemental carbon: the EUSAAR protocol, Atmos. Meas. Tech., 3(1), 79–89, doi:10.5194/amt-3-79-2010, 2010.

Ceburnis, D., Masalaite, A., Ovadnevaite, J., Garbaras, A., Remeikis, V., Maenhaut, W., Claeys, M., Sciare, J., Baisnée, D. and O'Dowd, C. D.: Stable isotopes measurements reveal dual carbon pools contributing to organic matter enrichment in marine aerosol, Sci. Rep., 6(July), 1–6, doi:10.1038/srep36675, 2016.

Chave, K. E.: Carbonates: Association with organic matter in surface seawater, Science (80-.)., 148(June), 1723–1724, doi:doi:10.1126/science.148.3678.1723, 1965.

Chave, K. E. and Suess, E.: Calcium Carbonate Saturation in Seawater: Effects of Dissolved Organic Matter, Limnol. Oceanogr., 15(4), 633–637, doi:10.4319/lo.1970.15.4.0633, 1970.

Chen, B., Cui, X. and Wang, Y.: Regional prediction of carbon isotopes in soil carbonates for Asian dust source tracer, Atmos. Environ., 142, 1–8, doi:10.1016/j.atmosenv.2016.07.029, 2016.

Chen, P., Kang, S., Abdullaev, S. F., Safarov, M. S., Huang, J., Hu, Z., Tripathee, L. and Li, C.: Significant influence of carbonates on determining organic carbon and black carbon: A case study in Tajikistan, central Asia, Environ. Sci. Technol., 55(5), 2839–2846, doi:10.1021/acs.est.0c05876, 2021.

477 Chow, J. C., Watson, J. G., Pritchett, L. C., Pierson, W. R., Frazier, C. A. and Purcell, R. G.: The dri thermal/optical
478 reflectance carbon analysis system: description, evaluation and applications in U.S. Air quality studies, Atmos.
479 Environ., 27A(8), 1185–1201, 1993.

480 Chow, J. C., Watson, J. G., Chen, L.-W. A., Chang, M. C. O., Robinson, N. F., Trimble, D. and Kohl, S.: The
481 IMPROVE_A temperature protocol for thermal/optical carbon analysis: maintaining consistency with a long-term
482 database., J. Air Waste Manage. Assoc., 57(9), 1014–1023, doi:10.3155/1047-3289.57.9.1014, 2007.

483 Descolas-Gros, C. and Fontugne, M.: Stable carbon isotope fractionation by marine phytoplankton during
484 photosynthesis, Plant. Cell Environ., 13(3), 207–218, doi:10.1111/j.1365-3040.1990.tb01305.x, 1990.

485 England, M. R., Eisenman, I., Lutsko, N. J. and Wagner, T. J. W.: The Recent Emergence of Arctic Amplification,
486 Geophys. Res. Lett., 48(15), 1–10, doi:10.1029/2021GL094086, 2021.

487 Feltracco, M., Barbaro, E., Spolaor, A., Vecchiato, M., Callegaro, A., Burgay, F., Vardè, M., Maffezzoli, N., Dallo,
488 F., Scoto, F., Zangrando, R., Barbante, C. and Gambaro, A.: Year-round measurements of size-segregated low
489 molecular weight organic acids in Arctic aerosol, Sci. Total Environ., 763, 142954,
490 doi:10.1016/j.scitotenv.2020.142954, 2021.

491 Flanner, M. G., Zender, C. S., Randerson, J. T. and Rasch, P. J.: Present-day climate forcing and response from
492 black carbon in snow, J. Geophys. Res., 112(D11), D11202, doi:10.1029/2006JD008003, 2007.

493 Friman, M., Aurela, M., Saarnio, K., Teinilä, K., Kesti, J., Harni, S. D., Saarikoski, S., Hyvärinen, A. and Timonen,
494 H.: Long-term characterization of organic and elemental carbon at three different background areas in northern
495 Europe, Atmos. Environ., 310(February), doi:10.1016/j.atmosenv.2023.119953, 2023.

496 Gensch, I., Kiendler-Scharr, A. and Rudolph, J.: Isotope ratio studies of atmospheric organic compounds: Principles,
497 methods, applications and potential, Int. J. Mass Spectrom., 365–366, 206–221, doi:10.1016/j.ijms.2014.02.004,
498 2014.

499 Groot Zwaaftink, C. D., Grythe, H., Skov, H. and Stohl, A.: Substantial contribution of northern high-latitude
500 sources to mineral dust in the Arctic, J. Geophys. Res., 121(22), 13,678-13,697, doi:10.1002/2016JD025482, 2016.

501 Gu, W., Xie, Z., Wei, Z., Chen, A., Jiang, B., Yue, F. and Yu, X.: Marine Fresh Carbon Pool Dominates Summer
502 Carbonaceous Aerosols Over Arctic Ocean, J. Geophys. Res. Atmos., 128(8), doi:10.1029/2022JD037692, 2023.

503 Hasegawa, S.: Experimental Characterization of PM2.5 Organic Carbon by Using Carbon-fraction Profiles of
504 Organic Materials, Asian J. Atmos. Environ., 16(2), 2021128, doi:10.5572/ajae.2021.128, 2022.

505 Holtz, L. M., Wolf-Gladrow, D. and Thoms, S.: Stable carbon isotope signals in particulate organic and inorganic
506 carbon of coccolithophores – A numerical model study for Emiliania huxleyi, J. Theor. Biol., 420(January), 117–
507 127, doi:10.1016/j.jtbi.2017.01.030, 2017.

508 Hu, Z., Kang, S., Xu, J., Zhang, C., Li, X., Yan, F., Zhang, Y., Chen, P. and Li, C.: Significant overestimation of

509 black carbon concentration caused by high organic carbon in aerosols of the Tibetan Plateau, Atmos. Environ.,
510 294(June 2022), 119486, doi:10.1016/j.atmosenv.2022.119486, 2023.

511 Huang, L., Brook, J. R., Zhang, W., Li, S. M., Graham, L., Ernst, D., Chivulescu, A. and Lu, G.: Stable isotope
512 measurements of carbon fractions (OC/EC) in airborne particulate: A new dimension for source characterization and
513 apportionment, Atmos. Environ., 40(15), 2690–2705, doi:10.1016/j.atmosenv.2005.11.062, 2006.

514 Huang, L., Zhang, W., Santos, G. M., Rodríguez, B. T., Holden, S. R., Vetro, V. and Czimczik, C. I.: Application of
515 the ECT9 protocol for radiocarbon-based source apportionment of carbonaceous aerosols, Atmos. Meas. Tech.,
516 14(5), 3481–3500, doi:10.5194/amt-14-3481-2021, 2021.

517 Jankowski, N., Schmidl, C., Marr, I. L., Bauer, H. and Puxbaum, H.: Comparison of methods for the quantification
518 of carbonate carbon in atmospheric PM10 aerosol samples, Atmos. Environ., 42(34), 8055–8064,
519 doi:10.1016/j.atmosenv.2008.06.012, 2008.

520 Karanasiou, A., Diapouli, E., Cavalli, F., Eleftheriadis, K., Viana, M., Alastuey, A., Querol, X. and Reche, C.: On
521 the quantification of atmospheric carbonate carbon by thermal/optical analysis protocols, Atmos. Meas. Tech., 4,
522 2409–2419, doi:10.5194/amt-4-2409-2011, 2011.

523 Kawai, K., Matsui, H. and Tobo, Y.: Dominant Role of Arctic Dust With High Ice Nucleating Ability in the Arctic
524 Lower Troposphere, Geophys. Res. Lett., 50(8), 1–10, doi:10.1029/2022GL102470, 2023.

525 Kawamura, K. and Watanabe, T.: Determination of stable carbon isotopic compositions of low molecular weight
526 dicarboxylic acids and ketocarboxylic acids in atmospheric aerosol and snow samples, Anal. Chem., 76(19), 5762–
527 5768, doi:10.1021/ac049491m, 2004.

528 Kawamura, K., Yanase, A., Eguchi, T., Mikami, T. and Barrie, L. A.: Enhanced atmospheric transport of soil
529 derived organic matter in spring over the Arctic, Geophys. Res. Lett., 23(25), 3735–3738, doi:10.1029/96GL03537,
530 1996.

531 Laskin, A., Laskin, J. and Nizkorodov, S. A.: Chemistry of Atmospheric Brown Carbon, Chem. Rev., 115(10),
532 4335–4382, doi:10.1021/cr5006167, 2015.

533 Liu, D., He, C., Schwarz, J. P. and Wang, X.: Lifecycle of light-absorbing carbonaceous aerosols in the atmosphere,
534 npj Clim. Atmos. Sci., 3(1), doi:10.1038/s41612-020-00145-8, 2020.

535 Mbengue, S., Zikova, N., Schwarz, J., Vodička, P., Šmejkalová, A. H. and Holoubek, I.: Mass absorption cross-
536 section and absorption enhancement from long term black and elemental carbon measurements: A rural background
537 station in Central Europe, Sci. Total Environ., 794, doi:10.1016/j.scitotenv.2021.148365, 2021.

538 McClelland, H. L. O., Bruggeman, J., Hermoso, M. and Rickaby, R. E. M.: The origin of carbon isotope vital effects
539 in coccolith calcite, Nat. Commun., 8(May 2016), 1–16, doi:10.1038/ncomms14511, 2017.

540 Meinander, O., Dagsson-Waldhauserova, P., Amosov, P., Aseyeva, E., Atkins, C., Baklanov, A., Baldo, C., Barr, S.

541 L., Barzycka, B., Benning, L. G., Cvetkovic, B., Enchilik, P., Frolov, D., Gassó, S., Kandler, K., Kasimov, N.,

542 Kavan, J., King, J., Koroleva, T., Krupskaya, V., Kulmala, M., Kusiak, M., Lappalainen, H. K., Laska, M., Lasne, J.,

543 Lewandowski, M., Luks, B., Mcquaid, J. B., Moroni, B., Murray, B., Möhler, O., Nawrot, A., Nickovic, S., O'neill,

544 N. T., Pejanovic, G., Popovicheva, O., Ranjbar, K., Romanias, M., Samonova, O., Sanchez-Marroquin, A.,

545 Schepanski, K., Semenkov, I., Sharapova, A., Shevnina, E., Shi, Z., Sofiev, M., Thevenet, F., Thorsteinsson, T.,

546 Timofeev, M., Umo, N. S., Uppstu, A., Urupina, D., Varga, G., Werner, T., Arnalds, O. and Vukovic Vimic, A.:

547 Newly identified climatically and environmentally significant high-latitude dust sources, Atmos. Chem. Phys.,

548 22(17), 11889–11930, doi:10.5194/acp-22-11889-2022, 2022.

549 Monteiro, F. M., Bach, L. T., Brownlee, C., Bown, P., Rickaby, R. E. M., Poulton, A. J., Tyrrell, T., Beaufort, L.,

550 Dutkiewicz, S., Gibbs, S., Gutowska, M. A., Lee, R., Riebesell, U., Young, J. and Ridgwell, A.: Why marine

551 phytoplankton calcify, Sci. Adv., 2(7), 1–14, doi:10.1126/sciadv.1501822, 2016.

552 Moschos, V., Dzepina, K., Bhattu, D., Lamkaddam, H., Casotto, R., Daellenbach, K. R., Canonaco, F., Rai, P., Aas,

553 W., Becagli, S., Calzolai, G., Eleftheriadis, K., Moffett, C. E., Schnelle-Kreis, J., Severi, M., Sharma, S., Skov, H.,

554 Vestenius, M., Zhang, W., Hakola, H., Hellén, H., Huang, L., Jaffrezo, J. L., Massling, A., Nøjgaard, J. K., Petäjä,

555 T., Popovicheva, O., Sheesley, R. J., Traversi, R., Yttri, K. E., Schmale, J., Prévôt, A. S. H., Baltensperger, U. and

556 El Haddad, I.: Equal abundance of summertime natural and wintertime anthropogenic Arctic organic aerosols, Nat.

557 Geosci., doi:10.1038/s41561-021-00891-1, 2022.

558 Mukherjee, P., Reinfelder, J. R. and Gao, Y.: Enrichment of calcium in sea spray aerosol in the Arctic summer

559 atmosphere, Mar. Chem., 227(May 2019), 103898, doi:10.1016/j.marchem.2020.103898, 2020.

560 Muller, A., Lamb, E. G. and Siciliano, S. D.: The silent carbon pool: Cryoturbic enriched organic matter in Canadian

561 High Arctic semi-deserts, Geoderma, 415(September 2021), 115781, doi:10.1016/j.geoderma.2022.115781, 2022.

562 Narukawa, M., Kawamura, K., Li, S.-M. and Bottenheim, J. W.: Stable carbon isotopic ratios and ionic composition

563 of the high-Arctic aerosols: An increase in δ^{13} C values from winter to spring, J. Geophys. Res., 113(D2), D02312,

564 doi:10.1029/2007JD008755, 2008.

565 Not, C. and Hillaire-Marcel, C.: Enhanced sea-ice export from the Arctic during the Younger Dryas, Nat. Commun.,

566 3(April 2014), 645–647, doi:10.1038/ncomms1658, 2012.

567 Okada, H. and Honjo, S.: Distribution of Oceanic Coccolithophorids in the Pacific., Deep Sea Res, 20(4), 355–374,

568 doi:10.1016/0011-7471(73)90059-4, 1973.

569 Petit, J. E., Favez, O., Albinet, A. and Canonaco, F.: A user-friendly tool for comprehensive evaluation of the

570 geographical origins of atmospheric pollution: Wind and trajectory analyses, Environ. Model. Softw., 88, 183–187,

571 doi:10.1016/j.envsoft.2016.11.022, 2017.

572 Petzold, A., Ogren, J. A., Fiebig, M., Laj, P., Li, S. M., Baltensperger, U., Holzer-Popp, T., Kinne, S., Pappalardo,

573 G., Sugimoto, N., Wehrli, C., Wiedensohler, A. and Zhang, X. Y.: Recommendations for reporting black carbon

574   measurements, Atmos. Chem. Phys., 13(16), 8365–8379, doi:10.5194/acp-13-8365-2013, 2013.

575   Phillips, R. L. and Grantz, A.: Regional variations in provenance and abundance of ice-rafted clasts in Arctic Ocean

576   sediments: Implications for the configuration of late Quaternary oceanic and atmospheric circulation in the Arctic,

577   Mar. Geol., 172(1–2), 91–115, doi:10.1016/S0025-3227(00)00101-8, 2001.

578   Pushkareva, E., Johansen, J. R. and Elster, J.: A review of the ecology, ecophysiology and biodiversity of

579   microalgae in Arctic soil crusts, Polar Biol., 39(12), 2227–2240, doi:10.1007/s00300-016-1902-5, 2016.

580   Raman, R. S., Ramachandran, S. and Kedia, S.: A methodology to estimate source-specific aerosol radiative forcing,

581   J. Aerosol Sci., 42(5), 305–320, doi:10.1016/j.jaerosci.2011.01.008, 2011.

582   Rodríguez, B. T., Huang, L., Santos, G. M., Zhang, W., Vetro, V., Xu, X., Kim, S. and Czimczik, C. I.: Seasonal

583   Cycle of Isotope-Based Source Apportionment of Elemental Carbon in Airborne Particulate Matter and Snow at

584   Alert, Canada, J. Geophys. Res. Atmos., 125(23), 1–15, doi:10.1029/2020JD033125, 2020.

585   Savadkoohi, M., Pandolfi, M., Favez, O., Putaud, J. P., Eleftheriadis, K., Fiebig, M., Hopke, P. K., Laj, P.,

586   Wiedensohler, A., Alados-Arboledas, L., Bastian, S., Chazeau, B., María, Á. C., Colombi, C., Costabile, F., Green,

587   D. C., Hueglin, C., Liakakou, E., Luoma, K., Listrani, S., Mihalopoulos, N., Marchand, N., Močnik, G., Niemi, J.

588   V., Ondráček, J., Petit, J. E., Rattigan, O. V., Reche, C., Timonen, H., Titos, G., Tremper, A. H., Vratolis, S.,

589   Vodička, P., Funes, E. Y., Zíková, N., Harrison, R. M., Petäjä, T., Alastuey, A. and Querol, X.: Recommendations

590   for reporting equivalent black carbon (eBC) mass concentrations based on long-term pan-European in-situ

591   observations, Environ. Int., 185(December 2023), 108553, doi:10.1016/j.envint.2024.108553, 2024.

592   Sharma, S., Lavoué, D., Chachier, H., Barrie, L. A. and Gong, S. L.: Long-term trends of the black carbon

593   concentrations in the Canadian Arctic, J. Geophys. Res. D Atmos., 109(15), 1–10, doi:10.1029/2003JD004331,

594   2004.

595   Sharma, S., Leaitch, W. R., Huang, L., Veber, D., Kolonjari, F., Zhang, W., Hanna, S. J., Bertram, A. K. and Ogren,

596   J. A.: An evaluation of three methods for measuring black carbon in Alert, Canada, Atmos. Chem. Phys., 17(24),

597   15225–15243, doi:10.5194/acp-17-15225-2017, 2017.

598   Sharma, S., Barrie, L. A., Magnusson, E., Brattström, G., Leaitch, W. R., Steffen, A. and Landsberger, S.: A Factor

599   and Trends Analysis of Multidecadal Lower Tropospheric Observations of Arctic Aerosol Composition, Black

600   Carbon, Ozone, and Mercury at Alert, Canada, J. Geophys. Res. Atmos., 124(24), 14133–14161,

601   doi:10.1029/2019JD030844, 2019.

602   Sirois, A. and Barrie, L. A.: Arctic lower tropospheric aerosol trends and composition at Alert, Canada: 1980-1995,

603   J. Geophys. Res., 104(D9), 11599–11618, 1999.

604   Smith, H. E. K., Tyrrell, T., Charalampopoulou, A., Dumousseaud, C., Legge, O. J., Birchenough, S., Pettit, L. R.,

605   Garley, R., Hartman, S. E., Hartman, M. C., Sagoo, N., Daniels, C. J., Achterberg, E. P. and Hydes, D. J.:

606   Predominance of heavily calcified coccolithophores at low CaCO3 saturation during winter in the Bay of Biscay,

607 Proc. Natl. Acad. Sci. U. S. A., 109(23), 8845–8849, doi:10.1073/pnas.1117508109, 2012.

608 Stein, A. F., Draxler, R. R., Rolph, G. D., Stunder, B. J. B., Cohen, M. D. and Ngan, F.: NOAA's HYSPLIT
609 atmospheric transport and dispersion modeling system, Bull. Am. Meteorol. Soc., 96(12), 2059–2077,
610 doi:10.1175/BAMS-D-14-00110.1, 2015.

611 Stein, R., Grobe, H. and Wahsner, M.: Organic carbon, carbonate, and clay mineral distributions in eastern central
612 Arctic Ocean surface sediments, Mar. Geol., 119(3–4), 269–285, doi:10.1016/0025-3227(94)90185-6, 1994.

613 Stjern, C. W., Samset, B. H., Myhre, G., Bian, H., Chin, M., Davila, Y., Dentener, F., Emmons, L., Flemming, J.,
614 Haslerud, A. S., Henze, D., Jonson, J. E., Kucsera, T., Lund, M. T., Schulz, M., Sudo, K., Takemura, T. and Tilmes,
615 S.: Global and regional radiative forcing from 20 % reductions in BC, OC and SO4 - An HTAP2 multi-model study,
616 Atmos. Chem. Phys., 16(21), 13579–13599, doi:10.5194/acp-16-13579-2016, 2016.

617 Toom-Sauntry, D. and Barrie, L. A.: Chemical composition of snowfall in the high Arctic: 1990-1994, Atmos.
618 Environ., 36(15–16), 2683–2693, doi:10.1016/S1352-2310(02)00115-2, 2002.

619 Verwega, M. T., Somes, C. J., Schartau, M., Tuerena, R. E., Lorrain, A., Oschlies, A. and Slawig, T.: Description of
620 a global marine particulate organic carbon-13 isotope data set, Earth Syst. Sci. Data, 13(10), 4861–4880,
621 doi:10.5194/essd-13-4861-2021, 2021.

622 Vodička, P., Kawamura, K., Schwarz, J. and Ždímal, V.: Seasonal changes in stable carbon isotopic composition in
623 the bulk aerosol and gas phases at a suburban site in Prague, Sci. Total Environ., 803, 149767,
624 doi:10.1016/j.scitotenv.2021.149767, 2022.

625 Wang, H. and Kawamura, K.: Stable carbon isotopic composition of low-molecular-weight dicarboxylic acids and
626 ketoacids in remote marine aerosols, J. Geophys. Res. Atmos., 111(7), doi:10.1029/2005JD006466, 2006.

627 Winiger, P., Barrett, T. E., Sheesley, R. J., Huang, L., Sharma, S., Barrie, L. A., Yttri, K. E., Evangeliou, N.,
628 Eckhardt, S., Stohl, A., Klimont, Z., Heyes, C., Semiletov, I. P., Dudarev, O. V., Charkin, A., Shakhova, N.,
629 Holmstrand, H., Andersson, A. and Gustafsson: Source apportionment of circum-Arctic atmospheric black carbon
630 from isotopes and modeling, Sci. Adv., 5(2), 1–10, doi:10.1126/sciadv.aau8052, 2019.

631 Zeebe, R. E.: History of seawater carbonate chemistry, atmospheric CO2, and ocean acidification, Annu. Rev. Earth
632 Planet. Sci., 40, 141–165, doi:10.1146/annurev-earth-042711-105521, 2012.

633